Epigenetic dynamics in meniscus cell migration and its zonal dependency in response to inflammatory conditions

Cite as: APL Bioeng. **9**, 016109 (2025); doi: 10.1063/5.0239035
Submitted: 16 September 2024 · Accepted: 7 February 2025 ·
Published Online: 20 February 2025

Yize Zhang,[1,2] Ellen Y. Zhang,[1,2] Catherine Cheung,[1,2] Yuna Heo,[1,2] Bat-Ider Tumenbayar,[3] Se-Hwan Lee,[1] Yongho Bae,[4,5] and Su Chin Heo[1,2,a)]

AFFILIATIONS

[1]McKay Orthopaedic Research Laboratory, Department of Orthopaedic Surgery, Perelman School of Medicine, University of Pennsylvania, Philadelphia, Pennsylvania 19104, USA
[2]Department of Bioengineering, School of Engineering and Applied Science, University of Pennsylvania, Philadelphia, Pennsylvania 19104, USA
[3]Department of Pharmacology and Toxicology, Jacobs School of Medicine and Biomedical Sciences, University at Buffalo, Buffalo, New York 14203, USA
[4]Department of Pathology and Anatomical Sciences, Jacobs School of Medicine and Biomedical Sciences, University at Buffalo, Buffalo, New York 14203, USA
[5]Department of Biomedical Engineering, School of Engineering and Applied Sciences, University at Buffalo, Buffalo, New York 14203, USA

[a)]**Author to whom correspondence should be addressed:** heosc@pennmedicine.upenn.edu

ABSTRACT

Meniscus injuries are challenging to treat due to the tissue heterogeneity and limited treatment efficacy. Understanding meniscus cell migration, crucial for healing, remains incomplete, especially its zonal dependency. This study explores how epigenetic mechanisms affect meniscus cell migration under inflammation, focusing on healing implications. Distinct histone modifications and chromatin dynamics between inner and outer cells were observed during migration, emphasizing the need to consider these differences in repair strategies. Furthermore, tumor necrosis factor alpha (TNF-α), a proinflammatory cytokine, slows inner meniscus cell migration, while outer cells remain unaffected, indicating a zonal response. Interestingly, TNF-α differentially alters histone modifications, particularly H3K27me3, between the cell types. Transcriptome analysis showed significant gene expression changes with inner cells more affected than outer cells. Gene cluster analysis revealed different responses in chromatin remodeling, extracellular matrix assembly, and wound healing between zones. We further identified potential therapeutic targets by using epigenetic drugs, GSKJ4 (a histone demethylase inhibitor) and C646 (a histone acetyltransferase inhibitor), which restored inner meniscus cell migration under inflammatory conditions, highlighting their potential in treating meniscus tears. This highlights their potential utility in treating meniscus tear injuries. Overall, our findings elucidate the intricate interplay between epigenetic mechanisms and meniscus cell migration, along with its meniscus zonal dependency. This study provides insight into potential targets for enhancing meniscus repair and regeneration, which may lead to improved clinical outcomes for patients with meniscus injuries and osteoarthritis.

INTRODUCTION

The meniscus plays a crucial role in knee joint function, providing load-bearing support, shock absorption, and joint stability in the knee.[1–3] Prevalent among the middle-aged and elderly, meniscus injuries pose a considerable challenge, particularly within the avascular zone where intrinsic healing is limited.[4–6] Current treatment options often involve arthroscopic surgeries, including meniscectomy, which alleviate pain and prevent joint locking, but unfortunately, they many inadvertently hasten osteoarthritis progression.[7–9] Thus, elucidating the factors that govern meniscus repair and regeneration is crucial for devising effective therapies.

Pro-inflammatory cytokines, especially tumor necrosis factor alpha (TNF-α), are implicated in both meniscus injury[10] and osteoarthritis pathogenesis.[11] Studies have shown elevated TNF-α levels in synovial fluid post meniscus injury are associated with subsequent osteoarthritis.[12–14] Notably, TNF-α impedes the healing process of meniscus tissue post injury,[11,15] whereas its inhibition via receptor antagonists fosters integrative meniscus repair.[11] Nonetheless, existing studies often overlook the zonal-dependent mechanical and biological properties of the meniscus in understanding the impact of injury on cellular behaviors in the meniscus.

The meniscus is composed of zones with distinct characteristics: the peripheral one-third (outer zone) is vascularized, whereas the inner one-third (inner zone) is avascular.[16] This zonal variation in vascularity likely influences cellular behavior and the response to injury. Meniscus cells are commonly classified into fibroblast-like cells, chondrocyte-like cells, and intermediate cells exhibiting characteristics of both.[1,17,18] Specifically, outer zone cells are typically oval and fusiform in shape, resembling fibroblasts in both appearance and behavior, and are thus classified as fibroblast-like cells. In contrast, inner zone cells are rounder and exhibit chondrogenic characteristics, leading to their classification as chondrocyte-like cells.[17–19] Such phenotypic disparity leads to diverse extracellular matrix (ECM) compositions; the inner zone contains substantial amounts of both type-I and type-II collagen and higher aggrecan content, while the outer meniscus zone predominantly contains type-I collagen.[16,20–22] These zonal distinctions in ECM composition suggest that factors influencing meniscus repair and regeneration are zone dependent. Consequently, comprehending these zone-dependent differences is essential for developing effective repair and regeneration strategies.

Intrinsic healing of meniscus tears necessitates proper cell migration to the injury site, a process governed by intricate phenotypic and transcriptional changes, which are in turn tightly regulated by epigenetic modifications.[23–25] There is growing evidence that global histone reorganization, marked by alterations in chromatin condensation, is essential for efficient cell migration. These changes in chromatin structure facilitate the dynamic reconfiguration of the nucleus, thereby facilitating cellular movements during migration.[25–27] Advances in super-resolution microscopy such as stochastic optical reconstruction microscopy (STORM) have made it possible to visualize and quantify chromatin organization at the nanoscale.[26,28,29] Research employing STORM has demonstrated that a comprehensive reorganization of chromatin is necessary for meniscus cell migration within the dense fibrous networks of tissues.[26] However, the specific epigenetic mechanisms that drive the migration of meniscus cells, particularly the differential responses of inner and outer meniscus cells in response to injury and pro-inflammatory cytokines, remain to be elucidated. Trimethylation of Histone H3 lysine 27 (H3K27me3) is pivotal in orchestrating phenotypic and transcriptomic alterations, significantly impacting cell migration across diverse cell types.[23–25] The downregulation of H3K27me3 levels via siRNA-mediated knockdown of EZH2 (the enzyme responsible for this specific methylation as a subunit of the polycomb repressive complex 2) has been observed to modulate cell migration in fibroblasts, mesenchymal stem cells, epithelial cells, and cancer cells.[30–33] These observations highlight the regulatory importance of H3K27me3 in cell motility within various biological settings. However, the specific contributions of H3K27me3 to meniscus cell migration, particularly its role in cells from different zones of the meniscus before and after injury, remain to be fully elucidated.

Thus, the objective of this study is to investigate the impact and zonal dependency of epigenetic mechanisms on meniscus cell migration. We particularly aim to explore how inflammatory conditions modulate the migratory behaviors of inner and outer meniscus cells migration. Furthermore, we interrogate the epigenetic mechanisms by which inner and outer meniscus cells respond differently to proinflammatory cytokine TNF-α by focusing on discrepancies in histone modifications along with global chromatin reorganization. This research offers valuable insight into the intricate interplay between epigenetic factors, inflammation, and meniscus cell behavior. Furthermore, this study also highlights the therapeutic potential of epigenetic manipulation, as evidenced by the restoration of cell migration speed following the inhibition of specific histone modifiers. Taken together, our study demonstrates that the migratory capacity of inner meniscus cells can be restored under TNF-α treatment through the small molecule modulation of histone methylation. This suggests a promising direction for epigenetic-targeted therapies aimed at intrinsic meniscus regeneration amidst inflammatory conditions. By advancing our comprehension of the epigenetic regulation of meniscus cell migration and its zonal dependency, this study makes a significant contribution to the field of meniscus repair and regeneration.

RESULTS

Differential histone modification patterns and chromatin dynamics drive distinct migration behaviors in inner and outer meniscus cells

To assess the baseline migration behaviors of inner and outer meniscus cells, juvenile bovine meniscus inner and outer cells were seeded onto 12-well tissue culture plates, and a wound closure "scratch" assay was performed over a 12-h period [Figs. 1(a) and 1(b)]. The 12-h timeframe was specifically chosen to minimize the influence of cell proliferation on closure, as large-animal meniscus cells exhibit extremely low proliferation rates under standard cell culture conditions.[34–36] This ensured that the wound closure process primarily attributable to individual cell migration (supplementary material Fig. 1). Quantitative analysis showed that both inner and outer cells exhibited comparable migration speeds and wound closure rates at 12 h post-scratch [Fig. 1(c)].

Next, to explore the changes in histone modification landscapes during migration, we compared histone modification markers between cells at the leading edge ("Front") and those at the rear back ("Back") of the migration process [Fig. 1(d)]. This comparison aimed to discern histone modification differences between the cells actively migrating at the front and those lagging at the back. Notably, we observed that the intensity of H3K27me3 (trimethylation of lysine 27 on histone H3, a marker of repressed facultative heterochromatin predominantly localized within the nuclei; supplementary material Fig. 2) in inner cells at the migration "Front" was higher than that in inner cells at the migration "Back" 1-h post-scratch [Figs. 1(d) and 1(f)]. As migration progressed, the intensity of H3K27me3 gradually increased with cells further from the migration front eventually matching the intensity levels observed at the migration leading edge over the course of 12 h, suggesting dynamic shifts in histone modification patterns during migration [Figs. 1(e) and 1(f)]. More intriguingly, the baseline level of

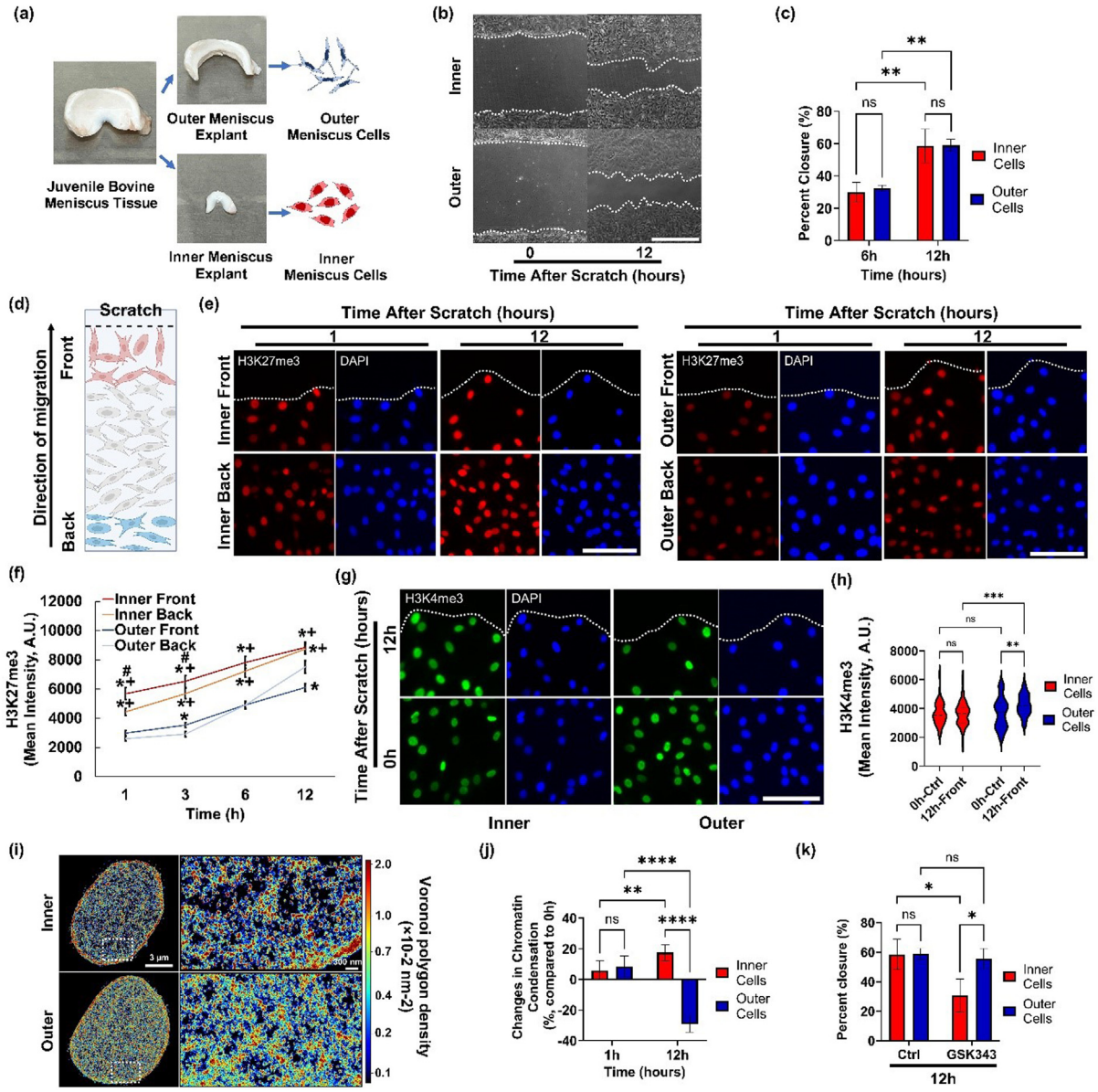

FIG. 1. H3K27me3 requires for inner meniscus cell migration: (a) Schematic illustrating isolation of inner and outer zone meniscus cells. (b) Representative images of wound closure assay in inner or outer meniscus cells (scale bar: 500 μm) and (c) results quantified as percent wound closure over time (3 different donors in triplicate, **: $p < 0.01$. Mean $\pm$ SD). (d) Schematic illustrating H3K27me3 immunofluorescence intensity measurement in inner or outer cells located at the migration front (Front) vs 10 cell layers behind the migration front (Back). Representative immunofluorescence images and quantifications of (e) and (f) H3K27me3 (*: $p < 0.05$ vs Outer Back, $+$: $p < 0.05$ vs Outer Front, #: $p < 0.05$ vs Inner Back, Mean $\pm$ SD), or (g) and (h) H3K4me3 (scale bar: 100 μm) after scratch ($n > 100$ cells/group, **: $p < 0.01$, ***: $p < 0.001$). (i) Representative H2B-STORM images and (j) percent change in chromatin condensation in nuclei at the migration "front" during migration ($n = 7$/group, **: $p < 0.01$, ****: $p < 0.0001$. Mean $\pm$ SD). (k) Comparison of inner vs outer meniscus cell migration with/without treatment with an EZH2 Inhibitor (GSK343, 10 μM, $n = 6$/group $*$: $p < 0.05$, Mean $\pm$ SD).

H3K27me3 in the inner cells was consistently higher than that in the outer cells throughout the migration [Figs. 1(e) and 1(f)]. Similarly, inner cells exhibited a higher average intensity of the heterochromatin marker H3K9me3 (tri-methylation of lysine 9 on histone H3, a repressed constitutive heterochromatin marker), although no significant changes in H3K9me3 levels were detected in either cell type during migration (supplementary material Fig. 3). There was no significant difference in the baseline intensity of the euchromatin marker H3K4me3 (tri-methylation of lysine 4 on histone H3, indicative of active euchromatin) between these cells ($p > 0.05$), with an observed

increase in intensity only in the outer cells during migration [Figs. 1(g) and 1(h)]. Similar changes were observed in H3K9ac (acetylation of lysine 9 on histone H3, an active euchromatin marker) throughout the migration process (supplementary material Fig. 4). These results point to distinct histone modification pattern alterations between inner and outer meniscus cell migration. Notably, H3K27me3 appears to play a more pronounced role in the migration of inner meniscus cells.

Upon noting the distinct roles of H3K27me3 in the migration of inner and outer meniscus cells, we further investigated differences in the global chromatin condensation level changes between these cell types during migration. Utilizing super-resolution stochastic optical reconstruction microscopy (STORM), we examined the nanoscale organization of histone H2B (H2B) to assess the global chromatin condensation in the nuclei of both cell types. For this, the inner and outer meniscus cells were fixed at short-term (1 h) and long-term (12 h) intervals post-scratch to trigger migration. Initial observations at 1-h post-scratch indicated increased chromatin condensation levels at the migration front in both inner and outer cells, suggesting that chromatin condensation is an early event in cell migration for both cell types [Figs. 1(i) and 1(j)]. However, interestingly, long-term observations at 12 h revealed sustained chromatin condensation in inner cells, whereas outer cells exhibited a significant reduction in chromatin condensation compared to both control and inner cells [Figs. 1(i) and 1(j)]. This indicates a differential regulation of chromatin dynamics during extended migration periods in these cell populations.

Building on the observed changes in histone methylation during the cell migration, we further investigated the necessity of H3K27me3 (the histone modification with significant changes during migration and marked differences between inner and outer cells) for proper cell migration. For this, we utilized GSK343, a selective inhibitor of Enhancer of Zeste Homolog 2 (EZH2), which catalyzes the methylation of lysine 27 on histone H3. GSK343 was administered to both inner and outer cells approximately 12 h prior to creating the scratch, and its presence was maintained during migration induction. The impact of EZH2 inhibition on cell migration was assessed using the wound closure assay (WCA). Intriguingly, while GSK343 treatment reduced the migration speed of inner meniscus cells, it did not affect the migration speed of outer meniscus cell [Fig. 1(k)]. These findings imply that H3K27me3 and its associated chromatin condensation play a more specific role in the regulation of inner meniscus cell migration.

Zone-dependent effects of inflammation on meniscus cell migration via nanoscale histone reorganization

Given the known inflammatory responses triggered by meniscal injury,[12–14] which influence migratory behavior of endogenous meniscus cells,[11,15] we further investigated the impact of TNF-α, a key pro-inflammatory cytokine, on the migration of meniscus cells. For this, juvenile bovine meniscus cells from the inner and outer zones were cultured in 12-well cell culture plates to 80% confluency before the pre-treatment with TNF-α overnight. Subsequently, a wound closure assay (WCA) was performed, and cell migration was visually assessed 12 h post-induction [Fig. 2(a)]. Notably, TNF-α treatment markedly reduced the migration speed of exclusively the inner zone cells, whereas the outer zone cells' migration remained unaffected when compared to the untreated control groups (Ctrl) [Figs. 2(b) and 2(c)]. These findings suggest zone-dependent responses of meniscus cells in response to inflammatory stimuli.

Observing that histone modification levels fluctuate during meniscus cell migration (Fig. 1), our subsequent analysis focused on the potential influence of TNF-α treatment on the migration velocity of meniscus cells via alterations in histone modification levels. To explore this, Inner and outer meniscus cells, cultured to 80% confluency, were subjected to fixation and staining for histone modification markers (H3K27me3, H3K9me3, and H3K4me3) following a 12-h exposure to TNF-α. Consistent with prior observations in Fig. 1, inner cells exhibited elevated baseline levels of the heterochromatin marker H3K27me3, which were notably diminished by TNF-α treatment—a response not mirrored in outer cells [Figs. 2(d) and 2(e)]. Conversely, the baseline levels of H3K9me3 were higher in inner cells, yet TNF-α treatment led to a reduction in both cell types, with outer cells experiencing a more pronounced decrease [Figs. 2(h) and 2(i)]. Interestingly, the euchromatin marker H3K4me3 displayed no initial disparity between cell types; however, TNF-α treatment resulted in an increase in inner cells and a decrease in outer cells [Figs. 2(f) and 2(g)]. These results suggest that TNF-α selectively modulates histone modification patterns in meniscus cells, particularly diminishing heterochromatin markers and augmenting euchromatin markers within inner cells. Further examination of global chromatin condensation levels during cell migration utilizing STORM-H2B imaging, revealed that inner cells at the migration forefront experienced a more substantial reduction in chromatin compaction following TNF-α treatment compared to outer cells (supplementary material Fig. 5). These findings indicate an overall trend wherein inner cells respond more sensitively to TNF-α treatment regarding H3K27me3 levels and chromatin condensation status, thereby experiencing a more significant decrease in migration speed under inflammatory conditions.

Transcriptomic divergence in inner and outer meniscus cells in response to TNF-α

Given the distinct impact of TNF-α on histone modifications and chromatin organization, influencing cell migration dynamics in inner and outer meniscus cells, we further hypothesized that TNF-α treatment would differentially alter the transcriptomic profiles in these cell populations. To explore this hypothesis, we performed a comprehensive whole-transcriptome analysis using mRNA samples from four experimental conditions: outer control (OC), outer TNF-α treatment (OT), inner control (IC), and inner TNF-α treatment (IT). By quantifying expression levels of 27 607 transcripts through next-generation sequencing, we aimed to uncover differences and commonalities across samples. Our unsupervised analysis, visualized via a principal component analysis plot (PCA, supplementary material Fig. 6) revealed that samples clustered primarily based on TNF-α treatment status along the PC1 axis, emphasizing the pivotal role of TNF-α in driving transcriptomic changes. Notably, within each treatment condition, the outer and inner meniscus samples exhibited distinct segregation along the PC2 axis, highlighting divergent transcriptomic responses to TNF-α treatment in these two cell subpopulations.

We further conducted a likelihood ratio test (LRT) with a stringent threshold of $p < 0.001$ to identify 2284 significantly altered transcripts across experimental conditions. To gain unbiased insight into the transcriptome alterations upon TNF-α treatment, we applied k-means clustering, an unsupervised machine learning method, on LRT-significant genes. K-means clustering divides data into k separate groups based on expression profile similarity, enabling us to identify

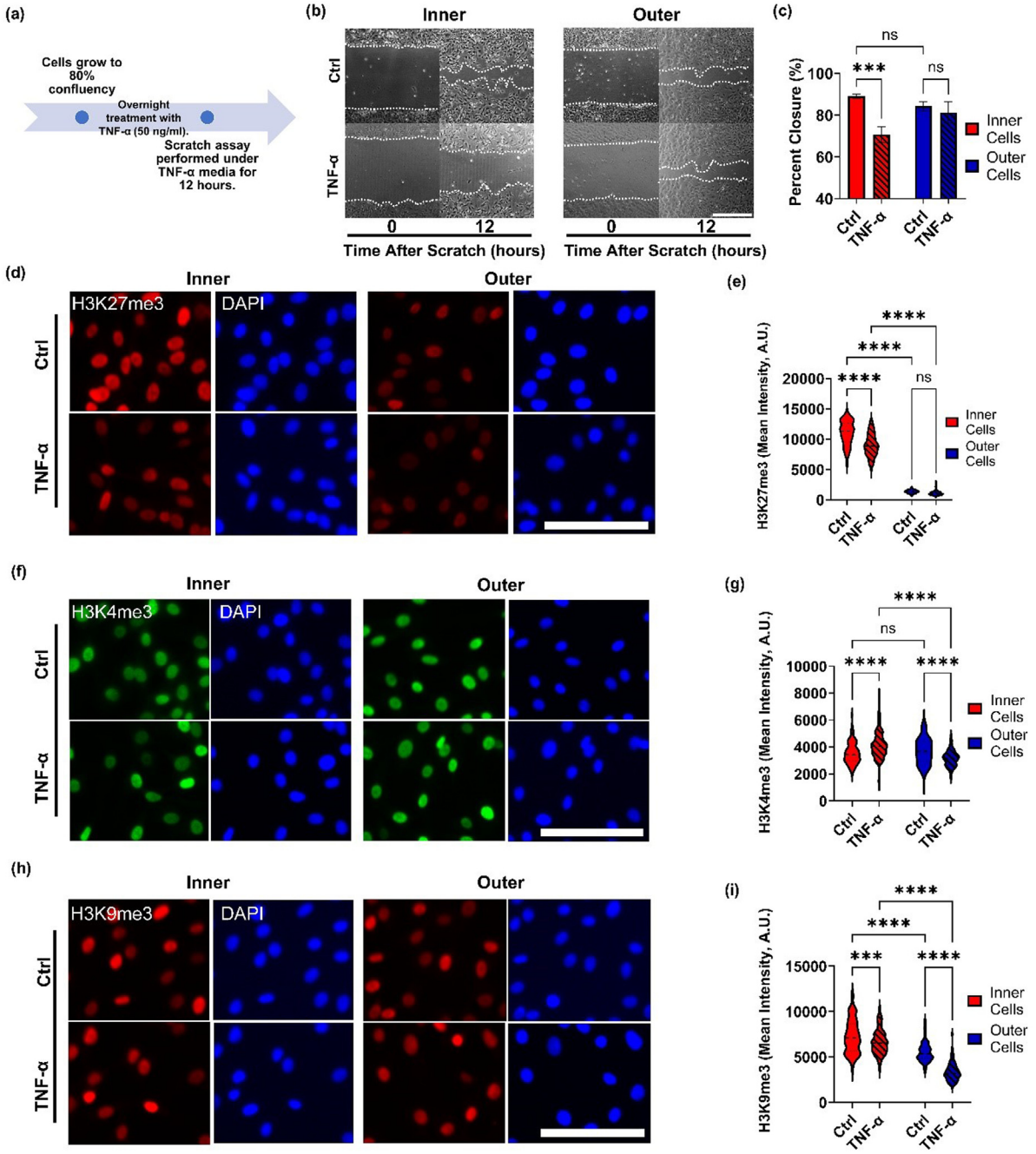

FIG. 2. TNF-α decreases inner but not outer meniscus cell migration speed via modulation of H3K27me3 levels. (a) Schematic showing the design of the TNF-α treatment study (12-h overnight treatment). (b) Representative images of wound closure assay (scale bar: 1 mm) and (c) results quantified as percent wound closure over time (performed in triplicate with cells from three different donors, ***: $p < 0.001$, Mean ± SD). Representative immunofluorescence images and quantifications of (d) and (e) H3K27me3, (f) and (g) H3K4me3, or (h) and (i) H3K9me3 (scale bar = 100 μm) in inner or outer meniscus cells treated with/without TNF-α (***: $p < 0.001$, ****: $p < 0.0001$, $n > 100$ cells/group).

different clusters with consistent gene expression patterns across samples without prior information. As shown in the heatmap [Fig. 3(a)], the k-means clustering divided the 2284 LRT-significant genes into six distinct clusters. Notably, clusters 1 and 5 exhibited divergent expression patterns in inner and outer meniscus cells following TNF-α treatment. To elucidate the functional relevance of these clusters, we performed gene ontology (GO) enrichment analysis. Cluster 1 was significantly enriched for biological processes related to chromatin

remodeling, cell cycle regulation, and protein localization to chromosomes [Fig. 3(b)]. This suggests distinct responses of inner and outer meniscus cells in these cellular processes upon TNF-α treatment. Furthermore, cluster 5 was enriched for processes associated with extracellular matrix assembly, wound healing, and cell migration [Fig. 3(c)]. Focusing specifically on cell migration-related genes, TNF-α treatment elicited distinct responses in inner vs outer meniscus cells. Inner meniscus cells exhibited more pronounced changes in migration-related gene expression levels compared to outer cells, indicating heightened sensitivity to TNF-α treatment [Fig. 3(d)]. Furthermore, TNF-α differentially regulated chondrogenic gene expression between inner cells (IC) and outer cells (OC), further emphasizing their distinct characteristics (supplementary material Fig. 7).

To further investigate the differential transcriptomic responses elicited by TNF-α treatment in inner and outer meniscus cells, we performed differential expression analysis and identified differentially expressed genes (DEGs). This analysis revealed a total of 1266 DEGs when comparing inner control (IC) vs inner tnf-α treatment (IT), with 785 genes upregulated and 481 genes downregulated [Fig. 3(e)]. Similarly, the comparison between outer control (OC) and outer TNF-α treatment (OT) identified 1082 DEGs, consisting of 710 upregulated and 372 downregulated genes [Fig. 3(f)]. Notably, an examination of the top 30 upregulated and downregulated genes indicated that over 50% of these genes exhibited divergent expression between the inner and outer meniscus cells (supplementary material Tables 1 and 2). These data indicate the unique transcriptomic changes induced by TNF-α treatment in each cell population, reflecting their distinct responses to inflammatory conditions.

Differential expression and distribution of TNF-α receptors in inner and outer meniscus cells

The distinct migration behaviors of inner and outer meniscus cells under TNF-α treatments led us to hypothesize that these differences might be attributed from variations in the presence of TNF-α receptors in these cells. Thus, we focused on two major TNF-α receptors, TNF-α receptor 1 (TNFR1) and TNF-α receptor 2 (TNFR2), both integral to cellular processes in mammalian cells. Employing macroscopic immunofluorescence and super-resolution STORM imaging, we compared the baseline levels of TNFR1 and TNFR2 in both cell types. Immunofluorescence analysis indicated a significantly higher intensity of TNFR1 in inner meniscus cells compared to outer cells [Figs. 4(a) and 4(b)]. Additionally, at the nanoscale level, we employed STORM imaging for cells fixed and stained with TNFR1 antibodies and then calculated the density of TNFR1 present on the cell membrane. Consistent with the immunofluorescence data, STORM images of TNFR1 revealed a significantly higher density in inner cells compared to outer cells [Figs. 4(c) and 4(e)]. We also observed that the TNFR2 expression was higher in inner compared to outer meniscus cells, though the differences are not as significant as those for TNFR1 (supplementary material Fig. 8). These findings suggest that the differential distribution and density of TNF surface receptors between the inner and outer meniscus cells contribute to the divergent responsiveness to TNF-α. Specifically, the higher levels and density of TNFR1 in inner meniscus cells may lead to more significant changes in histone modification and chromatin condensation levels, thereby influencing cell migration under inflammatory conditions.

Selective inhibition of histone enzyme activation restores TNF-α-mediated migration in inner meniscus cells

Recognizing the pivotal role of H3K27me3 in TNF-α-mediated reduction of inner meniscus cell migration speed, we next hypothesized that altering the histone methylation levels affected by TNF-α could potentially restore the impaired migration speed. To test this hypothesis in this study, we leveraged established epigenetic drugs targeting key histone modification processes. Specifically, we employed GSKJ4, an inhibitor of the H3K27me3 demethylase JMJD3, known to elevate the overall level of H3K27me3 in cells,[37–40] and C646, an inhibitor of the histone acetyltransferase p300, which reduces the overall level of histone acetylation.[41–43]

To evaluate the potential therapeutic strategies for meniscus healing, we evaluated the effects of GSKJ4 and C646 on the migration speed of inner meniscus cells under TNF-α-induced inflammatory conditions. Our wound closure assay results were promising, showing that a 12-h treatment with GSKJ4 at both low (2 μM, GSKL) and high doses (5 μM, GSKH) partially restored the migration capacity of TNF-α-treated inner meniscus cells [Figs. 5(a) and 5(c)]. Similarly, pretreatment with C646 at low (10 μM, C646L) and high doses (30 μM, C646H) also led to partial recovery in migration capacity under TNF-α treatment [Figs. 5(a) and 5(c)]. These findings suggest that the epigenetic modulation by GSKJ4 and C646 can effectively counteract the histone methylation alterations induced by TNF-α, potentially fostering a transcriptional environment conducive to cell migration. Considering the chronic inflammation and impaired healing associated with meniscal injuries, repurposing GSKJ4 and C646 emerge as a novel therapeutic approach to enhance recovery. Future studies should focus on the long-term effects of these treatments on meniscus cell behavior and their potential to enhance functional recovery *in vitro* and *in vivo*. Further exploration of the gene expression profiles and signaling pathways affected by these epigenetic drugs will provide insight into their mechanisms of action for developing targeted therapies for musculoskeletal injuries. Taken together, this study reveals that the modulation of histone methylation and acetylation can significantly influence the migratory behavior of meniscus cells, potentially offering new therapeutic intervention for enhancing tissue repair.

DISCUSSION

Meniscus injuries are common and challenging to treat, particularly in the avascular inner zone where current interventions like suturing or meniscectomy fall short. Thus, there is a pressing need for the development of new treatment methods. To address the unmet clinical needs, in this study, we aimed to investigate the impact of epigenetic mechanisms on meniscus cell migration under inflammatory conditions, and understand the differential histone modification patterns and chromatin dynamics driving distinct cell migration behaviors with the ultimate goal of pioneering epigenetic-based therapies for meniscus repair. Here, we established that the histone modification marker H3K27me3 plays a critical role in facilitating the proper migration of inner meniscus cells under inflammatory conditions. Furthermore, we elucidated the alterations in chromatin condensation and transcriptomic profiles that contribute to the observed migration pattern of inner meniscus cells.

Our objectives were to elucidate the epigenetic mechanisms influencing meniscus cell migration under inflammatory conditions

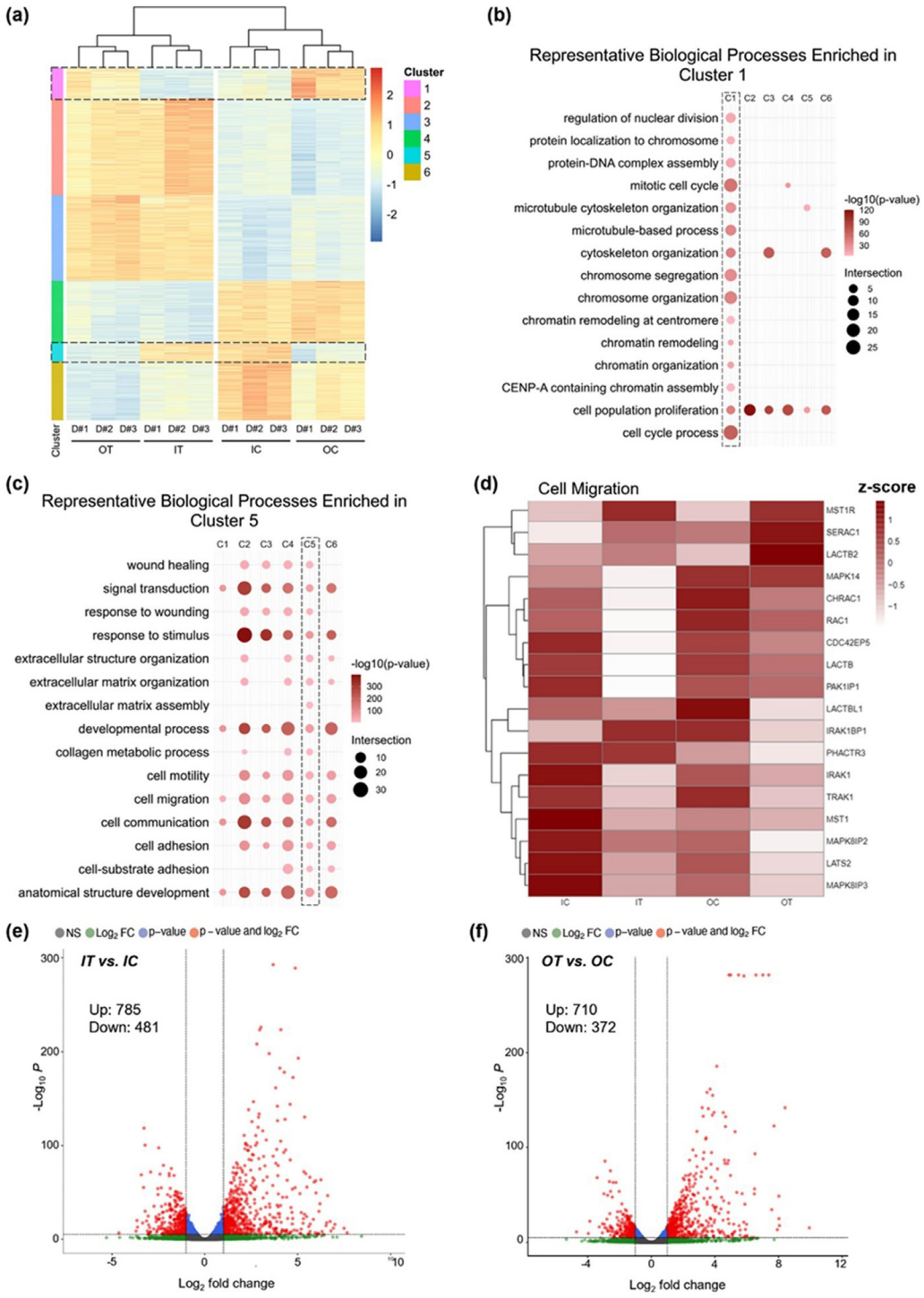

FIG. 3. Transcriptomic landscape alterations in inner and outer meniscus cells upon TNF-α treatment. (a) Heatmap displaying expression patterns and K-means clustering (six clusters) of 2284 likelihood ratio test (LRT)-significant genes ($p < 0.001$) across four conditions: outer control (OC), outer TNF-α (OT), inner control (IC), and inner TNF-α (IT). Bubble plots showing representative biological processes enriched in (b) cluster 1, related to chromatin remodeling, cell cycle, and protein localization to chromosomes, and (c) cluster 5, associated with extracellular matrix assembly, wound healing, and cell migration. Bubble size represents the number of genes associated with each process and color intensity shows significance level $-\log_{10}$(p-value). (d) Heatmap displaying expression pattern of cell migration-related genes across IC, IT, OC, and OT measured in Z-score. Volcano plots show the distributions of differentially expressed genes (DEGs) in (e) IT vs IC or (f) OT vs OC comparisons.

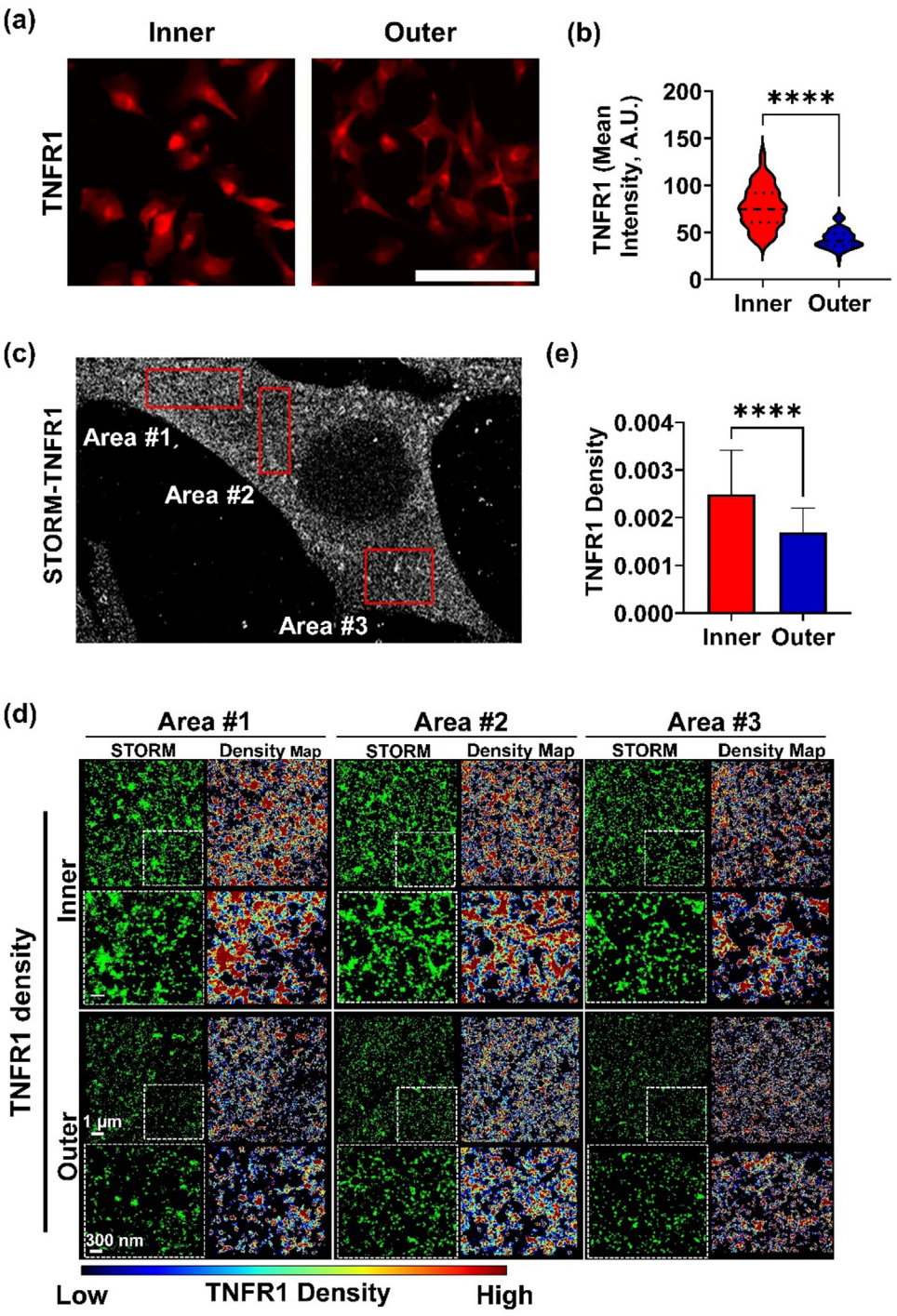

FIG. 4. Baseline TNFR1 expression is higher in inner cells compared to outer cells. (a) Representative immunofluorescence images of TNF-α Receptor 1 (TNFR1) in inner or outer cells (scale bar: 100 μm) and (b) quantification of TNFR1 intensity ($n > 100$ cells/group, ****: $p < 0.0001$). (c) Nanoscale TNFR1 distribution measured in three random areas per cell, and representative (d) TNFR1 STORM images and density map, and (e) quantifications of TNFR1 density (number of TNFR1 localizations per total area, demonstrating significantly higher density in inner cells, $n > 100$ measurements/group, mean ± SD).

and to explore therapeutic avenues for enhancing meniscus repair. To this end, we exposed inner and outer meniscus cells to TNF-α known to impede repair processes.[44–46] Notably, our experiments confirmed that TNF-α significantly curtails the migration speed of inner meniscus cells without affecting outer cells. This led us to probe deeper into the associated histone modification and transcriptomic changes. Consequently, we administered existing epigenetic drugs targeting histone acetyltransferase and histone demethylase to restore the migratory capability of inner meniscus cells under inflammatory conditions.

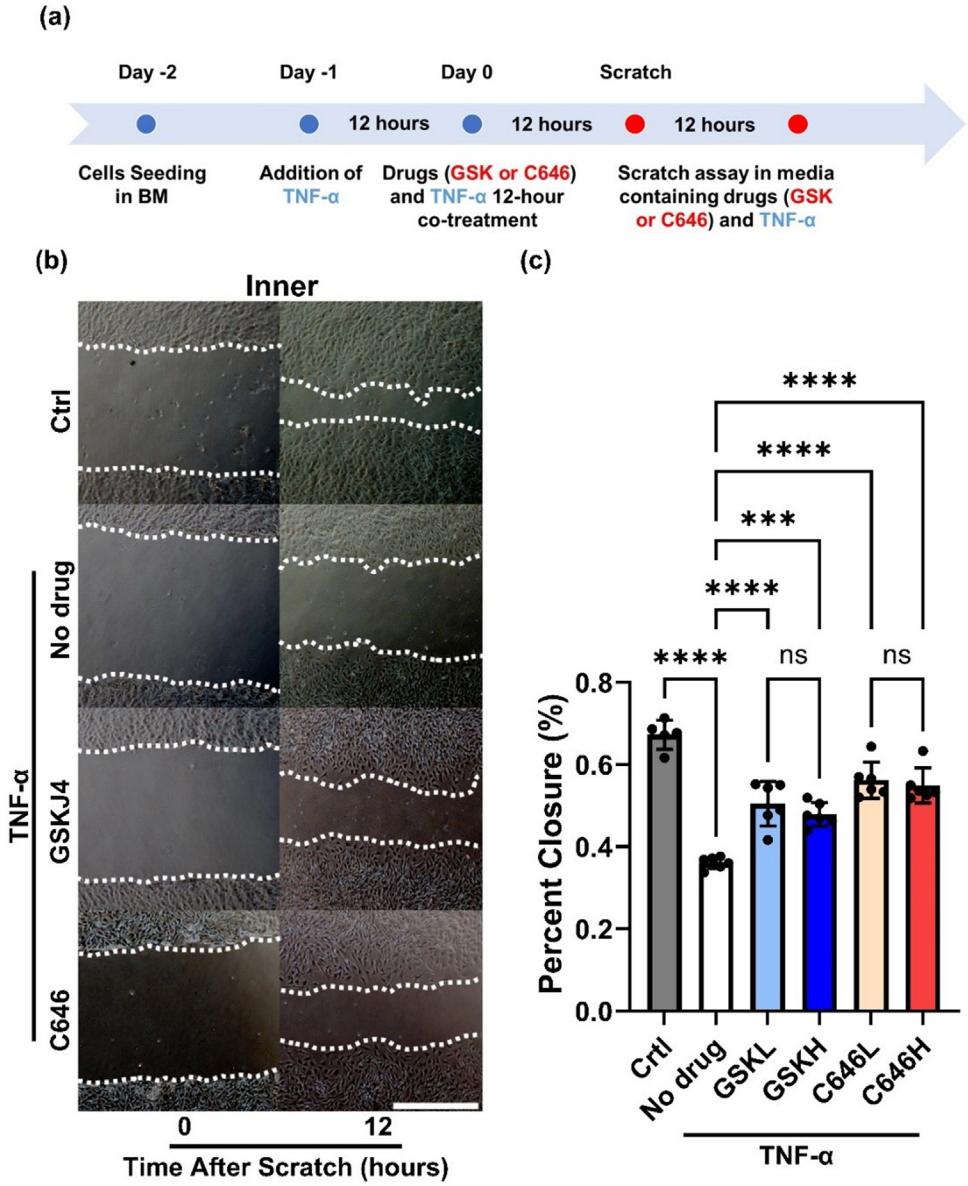

FIG. 5. GSKJ4 and C646 restore inner meniscus migration speed under TNF-α treatment. (a) Schematic illustrating the design of the epigenetic drug treatment study. Inner meniscus cells were subjected to TNF-α overnight treatment, followed by 12 h of co-treatment with TNF-α and epigenetic drugs before performing the 12-h scratch assay. (b) Wound closure assay images demonstrating the effects of drug treatments (scale bar = 1 mm). (c) Quantification of wound closure over time, expressed as percent wound closure (n = 5–6 per condition from three different donors; ***: $p < 0.001$, ****: $p < 0.0001$. Mean ± SD, L: low dose, H: high dose).

We discovered pronounced differences in histone modification patterns and chromatin organization between the two cell types during migration. Notably, inner meniscus cells exhibited higher levels of the heterochromatin marker H3K27me3 compared to outer meniscus cells during migration. The selective inhibition of EZH2, which aimed to reduce H3K27me3 levels, resulted in a decreased migration speed exclusively in inner cells, aligning with findings in other cell types.[30–33] Conversely, outer meniscus cells remained unresponsive to EZH2 inhibition, underscoring a specific regulatory role for H3K27me3 in inner cell migration. Furthermore, TNF-α treatment was found to selectively reduce H3K27me3 levels in inner cells. While the exact mechanism behind TNF-α's induction of zonal-dependent epigenetic changes is not fully understood, the differential response hints at distinct sensitivities to pro-inflammatory signals between inner and outer meniscus cells. This could be due to the higher density of TNF-α receptors on inner meniscus cells. These insights accentuate the importance of considering the zonal properties of the meniscus when addressing its inflammatory response. The zonal-dependent impact of TNF-α on

histone modifications could be pivotal in developing targeted therapies for meniscus injuries.

Our study elucidated differential changes in global chromatin condensation between inner and outer meniscus cells during extended migration. We observed that chromatin condensation in inner cells not only persisted but increased over time, whereas it decreased in outer cells. This observation supports the "pack and go" hypothesis, which posits that chromatin condensation is essential for initiating cell migration.[25–27] The sustained increase in chromatin condensation in inner cells may reflect enduring transcriptional changes linked to their migratory phenotype. Conversely, the reduction in chromatin condensation in outer cells could suggest a distinct transcriptional program that facilitates their migration. To understand the disparate epigenetic responses of inner and outer meniscus cells to TNF-α treatment, we analyzed the TNF surface receptors. Our findings indicate a higher abundance and density of TNF-α receptor 1 (TNFR1) in inner cells, correlating with the reduced migration speed under inflammatory conditions. The pronounced presence of TNFR1 implies a heightened sensitivity of inner cells to TNF-α, leading to downstream epigenetic alterations, particularly affecting H3K27me3 levels, which are crucial for the migration of inner meniscus cells.

To explore the cellular mechanisms driving changes in cell migration induced by inflammation, we employed RNA sequencing (RNA-seq) to profile transcriptomic alterations in response to TNF-α. Principal component analysis (PCA) identified TNF-α as a significant influencer of transcriptomic shifts, demonstrating the divergent transcriptomic responses between inner and outer meniscus cell populations. Employing a stringent Likelihood Ratio Test (LRT) and k-means clustering, we identified 2284 significantly altered transcripts and six distinct clusters with unique expression profiles. Notably, clusters pertinent to chromatin remodeling and cell migration displayed contrasting expression patterns between the two cell types. Interestingly, key cell migration-related genes such as MAPK14 and MAPK8IP3 were found to be downregulated in inner meniscus cells post-treatment, which are recognized for their role in promoting cell migration.[47] Additionally, genes associated with the Rho GTPase family, including Rac1 and CDC42EP5, exhibited reduced expression in inner cells, providing a potential mechanism underlying their diminished migration speed under inflammation conditions.[48] Additionally, the differential expression analysis revealed the distinct cellular mechanisms activated in each population. The variable regulation of chromatin dynamics emphasizes the meniscus's inherent heterogeneity, calling for tailored approaches to cater to the specific cellular responses during the healing process. Through the elucidation of these molecular pathways, our goal is to forge more effective methods for facilitating meniscus repair and regeneration, ultimately enhancing clinical outcomes for patients with meniscus injuries. These findings underscore the importance of accounting for zonal-dependent properties in meniscus repair and regeneration.

A significant accomplishment of this study is the novel application of existing epigenetic drugs for treating meniscus tear injuries. Our selected drug candidates, GSKJ4 (a histone demethylase inhibitor)[37–40] and C646 (a histone acetyltransferase inhibitor)[41–43] effectively restored the migration speed of the inner meniscus cells under TNF-α treatment. This aligns with prior research suggesting that inflammatory cytokines activate JMJD3 via the NF-kB pathway, diminishing H3K27me3 levels.[49] Both GSKJ4 and C646 have demonstrated anti-inflammatory effects in various models, linking their roles in limiting inflammation with promoting cell migration in meniscus cells.[50,51] Similarly, C646 has shown promise in alleviating inflammatory responses in conditions such as inflammatory lung disease[52] and anti-bacterial macrophages.[53]

Our study is the first to demonstrate that only inner meniscus cells modify key heterochromatin markers, particularly H3K27me3, in response to TNF-α, influencing their migration speed. While the epigenetic effects were observed using specific inhibitors, transgenic mouse models could offer significant insights into genetic and epigenetic mechanisms. Additionally, we chose bovine meniscus tissue for its closer anatomical and mechanical similarities to human menisci, which are critical for evaluating the translational potential of repair strategies. Furthermore, given the substantial differences in cell migration behavior between 2D and 3D environments, employing advanced 3D migration assays will be critical to validating the potential of anti-TNF-α therapies in meniscus tissue engineering. We also recognize that *in vivo* studies are necessary to strengthen our findings. Future work will incorporate animal models to assess the impact of epigenetic interventions on meniscus healing and repair. In addition, although the precise mechanisms by which H3K27me3 alterations regulate migration-related gene expression remain unclear, future research utilizing epigenetic sequencing techniques, such as ChIP-seq and ATAC-seq, will be essential for elucidating the epigenetic landscape governing cell migration. These efforts will help bridge the gap between basic science and clinical applications, enhancing the relevance of our findings for human treatments.

Finally, in this study, we focused on the primary cell types derived from the inner or outer meniscus; however, we acknowledge the limitations in identifying specific subpopulations within these regions. While fibroblast-like and chondrocyte-like cells are the primary cell types in the meniscus,[1,17,18] other minor cell types, such as endothelial cells and stem/progenitor cells, are also resided in the meniscus and play crucial roles in its repair.[36,54] Additionally, the findings presented in this study reflect the collective responses of mixed cell populations rather than isolated behaviors. Thus, future studies employing advanced techniques, such as single-cell RNA sequencing or flow cytometry, will be critical for isolating and characterizing these cell types to provide a more detailed understanding of their individual roles in meniscus regeneration. Despite these limitations, our findings indicate the importance of zonal differences in cellular phenotypes as key drivers of the observed epigenetic responses, emphasizing the need to consider zone-specific dynamics when developing targeted strategies for meniscus repair.

In conclusion, this study enhances our understanding of the interplay between epigenetic mechanisms, zonal-dependent properties, and meniscus cell migration. Our findings also highlight the importance of considering meniscus heterogeneity and provide insights into potential targets for improving meniscus repair and regeneration. These results suggest promising avenues for developing targeted interventions to enhance clinical outcomes for individuals with meniscus injuries and osteoarthritis. Further research is needed to elucidate the specific molecular mechanisms underlying the observed epigenetic changes and their functional consequences in meniscus repair and regeneration. The approach employed in this study also shows promise for treating injuries in other tissues, including tendon, muscle, cardiovascular, skin, and neural tissues, warranting further exploration.

METHODS

Meniscus cell isolation and culture

Inner and outer meniscus cells were isolated following previously established protocols.[18,26,34,55] Briefly, juvenile bovine menisci (<3 months, Research 87, Inc., Boylston, MA) were harvested and divided into the inner and outer meniscus areas. First, the superficial layers of the meniscus were removed. The inner one-third of the meniscus, characterized by its avascular and more transparent appearance, was sectioned into small cubes (approximately 1 mm^3) to isolate inner meniscus cells. Similarly, the outer one-third, which is less transparent and whiter in appearance, was cut, and the central portion of this section was diced into small cubes (approximately 1 mm^3) for outer meniscus cell extraction. [Fig. 1(a)]. The respective meniscus tissues were then cut into 5 mm cubes. To isolate meniscus cells,[18,26] the inner and outer meniscus tissue cubes were cultured separately in basal growth media consisted of Dulbecco's Modified Eagle's medium supplemented with 10% fetal bovine serum and 1% penicillin, streptomycin, and fungizone (PSF) in an incubator maintained at 37 °C and 5% CO_2 for approximately 14 days, after which inner and outer meniscus cells were collected. To ensure consistent cell conditions, only passage 1 (P1) cells were used for all subsequent experiments.

Wound closure assay

To assess 2D migration of inner and outer meniscus cells, a wound closure "scratch" assay (WCA) was conducted. Cells (at passage, P1) were seeded onto the twelve-well tissue culture dish (2×10^5 cells per well). The cells were cultured additionally for 1–2 days until they reached 90% confluency. Subsequently, the WCA was initiated by creating a scratch on the surface of the plate using a 20 μl standard pipette, forming one horizontal and one vertical scratch intersecting at the center of the plate. Images were captured using an Inverted Microscope (Nikon ECLIPSE TS100) at 0, 6, or 12 h post-scratch. The percent closure of the wound was determined by analyzing the images with ImageJ.

For the drug or pro-inflammatory cytokine treatments during the WCA, P1 cells were initially seeded in the twelve-well tissue culture dishes at a density of 2×10^5 cells per well and cultured until reaching 80% confluency (typically taking 1–2 days). To investigate the effect of the EZH2 inhibitor on cell migration speed, cells were then treated with GSK343 (SML0766-Sigma-Aldrich) at concentrations of 10 μM in BM overnight before conducting the "scratch" assays. To examine how the inflammatory cytokine TNF-α influences meniscus cell migration speed, cells were treated with TNF-α (T7539-Sigma-Aldrich) at concentrations of 50 ng/ml prior to the "scratch" assays [Fig. 3(a)].

To explore the potential of using existing small molecule histone modification drugs to restore inner meniscus cell migration speed under inflammatory conditions, cells were pretreated with TNF-α (T7539-Sigma-Aldrich) overnight before co-treatment with C646 (a histone acetyltransferase inhibitor, SML0002-Sigma Aldrich) at a concentration of 10 μM (Low dose, L) or 30 μM (High dose, H) or GSKJ4 (a histone demethyltransferase inhibitor, ab144395-Abcam) at concentration of 2 μM (L) or 5 μM (H) for 12 h prior to the scratch assay [Fig. 5(a)].

RNA-sequencing

To investigate the transcriptomic level changes leading to different responses to TNF-α between inner and outer meniscus cells, RNA sequencing was performed on both cell types with and without TNF-α treatment. Passage 1 (P1) cells were seeded in six-well tissue culture dishes at a density of 1×10^6 cells per well. The cells were cultured for an additional 1–2 days until they reached 90% confluency. For the control group, total RNA from inner and outer meniscus cells was collected after 2 days of culture using TRIzol Reagent (Invitrogen). For the TNF-α treatment group, cells were treated with TNF-α (T7539-Sigma-Aldrich) at a concentration of 50 ng/ml in 3 ml of BM overnight (12 h) before RNA collection using the same method. The collected RNA was purified using Direct-zol RNA Microprep Kits (Zymo Research). RNA sample quality was assessed with a NanoDrop Spectrophotometer (Thermo Fisher Scientific), a Qubit Fluorometer (Thermo Fisher Scientific), and an Agilent 2100 Bioanalyzer (Agilent Technologies). RNA-Seq library preparation (rRNA depletion) and sequencing (150 bp paired-end) were performed at Genewiz (South Plainfield, New Jersey). Sequence reads were trimmed to remove possible adapter sequences and low-quality nucleotides using Trimmomatic v.0.36. The trimmed reads were then mapped to the Bos taurus reference genome (available on Ensembl) using the STAR aligner v.2.5.2b. Unique gene hit counts were calculated using featureCounts from the Subread package v.1.5.2.

Differential expression analysis between the experimental conditions Outer Control (OC), Outer TNF-α (OT), Inner Control (IC), and Inner TNF-α (IT) was performed using the DESeq2 package of R programming language.[56] The EnhancedVolcano R package was used to visualize the global transcriptional change across the groups compared.[48] The DESeq2 Likelihood Ratio Test (LRT) was applied to test for differential expression between contrasts of interest. A stringent significance threshold of $p < 0.001$ was used for this analysis to ensure a robust level of confidence in the rejection of the null hypothesis. Additionally, the DESeq2 package was used to identify differentially expressed genes (DEGs). DEGs were selected based on the following thresholds: Benjamini-Hochberg adjusted p-value of <0.05, absolute log2(fold-change) of >1.0. R pheatmap package[57] was used to illustrate expression patterns, clusters, and distributions of LRT-significant genes.

To gain a deeper understanding of the functional profiling associated with LRT-significant genes, a gene enrichment analysis was performed to examine highly enriched biological processes. The analysis was carried out using the g:GOSt function on the gProfiler web server (https://biit.cs.ut.ee/gprofiler/gost).[58] The significance threshold was set to the Benjamini-Hochberg FDR (false discovery rate) value, and significant Gene Ontology (GO) terms were defined by an adjusted p value of ≤0.05. For visualization purpose, bubble plots for the representative GO terms were generated using the ggplot2 package of R.[59]

Immunofluorescence

To examine the dynamics of various histone modification markers during cell migration and drug treatments, cells were fixed with 4% paraformaldehyde for 20 min at 37 °C at different time points, specifically 1, 6, and 12 h after creating the scratch. Cells were permeabilized for 5 min in a solution of 0.05% Triton X-100 in PBS supplemented with 320 mM sucrose and 6 mM magnesium chloride.

For fluorescence labeling of histone modification markers, cells were incubated at 4 °C overnight with primary antibodies targeting H3K27me3 (Rabbit, 9733 CST, 1:300, Thermo), H3K9me3 (Mouse, 6F12 CST, 1:300, Thermo), and H3K4me3 (Rabbit, 9751 CST, 1:300, Thermo), H3K9ac (Rabbit, MA5-11195, 1:200, Thermo) in PBS. Cells

were then incubated for 60 min at room temperature with Alexa-Fluor goat anti-mouse or anti-rabbit secondary antibody (1:200; Thermo Fisher). Images were acquired using a widefield microscope (Leica DM6000) at 20× magnification and analyzed for fluorescence mean intensity at the migration front and migration back [Fig. 2(a)] using ImageJ.

To assess the effects of TNF-α treatment on histone modification marker expressions in inner and outer meniscus cells, inner and outer cells were seeded on 24 well-treated plates for 1–2 days were then treated with 50 ng/ml TNF-α (T7539-Sigma-Aldrich) overnight (12 h). Fixed cells were then stained and imaged for H3K27me3, H3K9me3, H3K4me3, or H3K9ac. Additionally, to investigate the distribution of the TNF-α surface receptors-1 or 2 (TNFR1 or TNFR2) on inner and outer meniscus cells, cells were fixed and stained with primary antibodies against TNFR1 (Rabbit, 1:200, ADI-CSA-815; ENZO) and TNFR2 (Rabbit, 1:200, ab15563; Abcam). Images were acquired using a widefield microscope (Leica DM6000) at 20× magnification and then analyzed for fluorescence mean intensity per cell using ImageJ.

STORM imaging

To investigate the effect of TNF-α treatment on chromatin condensation levels at the nanoscale in the cells, inner and outer meniscus cells were seeded on 8-well cover glass chambers (Nunc™ Lab-Tek™ II Chambered Coverglass) for 2 days in BM before conducting the WCA. TNF-α (50 ng/ml) was added to the chamber, and cells were treated overnight with TNF-α, followed by fixation with methanol-ethanol (1:1) at −20 °C for 7 min. To optimize antibody staining and minimize nonspecific bindings, a blocking buffer (BlockAid, ThermoFisher) was added to each well and incubated for 1 h. Diluted anti-histone H2B (Rabbit, 1:50, 15857-1-AP; Proteintech) was then added to the wells and incubated overnight at 4 °C to specifically label the H2B histone protein.

Following sample preparation, samples were washed and subsequently incubated for 40 min with secondary antibodies custom-labeled with activator-reporter dye pairs (Alexa Fluor 405–Alexa Fluor 647, Invitrogen) for STORM imaging.[26,28,29,60] All imaging experiments were conducted using a commercial STORM microscope system (ONI Nanoimager). During imaging, the 647-nm laser was utilized to excite the reporter dye (Alexa Fluor 647, Invitrogen) and switch it to the dark state. Subsequently, a 405-nm laser was employed to reactivate the Alexa Fluor 647 in an activator dye (Alexa Fluor 405)–facilitated manner. An imaging cycle was implemented in which one frame belonging to the activating light pulse (405 nm) was alternated with three frames belonging to the imaging light pulse (647 nm). To ensure proper photo-switching of the Alexa Fluor 647, an imaging buffer, prepared according to a previously established protocol,[26,28,29,60] was utilized. The imaging buffer comprised 10 mM cysteamine MEA (Sigma Aldrich, 30070–50 G), 0.5 mg/ml glucose oxidase, 40 mg/ml catalase (Sigma), and 10% glucose in PBS.[26,28,29,60] Cellular localization at the migration front was achieved using a 640 nm laser to excite the Alexa Fluor 647 dye, acquiring a total of 20,000 frames of images per nucleus. STORM image localizations were obtained using Nanoimager software (ONI) and rendered with custom-written software Insight3 (a gift from B. Huang, UCSF, USA). For quantitative analysis, custom-written MATLAB codes were employed.[26,28,29,60] TNFR1 nanoscale distribution was quantified via random sampling of three different locations on the cell surface (three locations covering approximately 50% of the cell area/cell), and then the ratio of localization/area (the number of localizations with detected localization/the total pixels in the sampled area) was analyzed [Fig. 4(c)].

Statistical analysis

Statistical analysis was conducted using GraphPad Prism 9 (La Jolla, CA). For comparisons between two groups, a Student's t-test was utilized, and two-way analysis of variance (ANOVA) with Tukey's honestly significantly different (HSD) post hoc test was used for multiple group comparisons. Transcriptomic data analysis was performed using the DESeq2 Likelihood Ratio Test (LRT) to assess differential expression between contrasts of interest, applying a significance threshold of $p < 0.001$, Benjamini-Hochberg adjusted p-value of < 0.05, and absolute log2(fold-change) of >1.0. The R pheatmap package was employed to visualize expression patterns, clusters, and distributions of LRT-significant genes, as well as the associated Gene Ontology terms. Results are presented as means ± SD, and differences were considered statistically significant at $p < 0.05$. Sample and replicate numbers are provided in the figure legends.

SUPPLEMENTARY MATERIAL

See the supplementary material for four additional figures and two tables for RNA-seq data.

ACKNOWLEDGMENTS

This research was supported by grants from the National Institutes of Health (Nos. K01 AR07787, R01 AR079224, and R01 HL163168) and the NSF Science and Technology Center for Engineering Mechanobiology (No. CMMI-1578571). We extend our gratitude to Dr. Robert L Mauck, Dr. Melike Lakadamyali, and Dr. Joel D. Boerckel for their invaluable scientific insights and contributions to this study.

AUTHOR DECLARATIONS

Conflict of Interest

The authors have no conflicts to disclose.

Ethics Approval

Ethics approval is not required.

Author Contributions

Yize Zhang: Conceptualization (equal); Data curation (lead); Formal analysis (lead); Investigation (lead); Methodology (lead); Validation (equal); Writing – original draft (equal); Writing – review & editing (equal). **Ellen Y. Zhang:** Conceptualization (supporting); Data curation (supporting); Formal analysis (supporting); Investigation (supporting); Methodology (supporting); Validation (supporting); Visualization (supporting); Writing – original draft (supporting); Writing – review & editing (supporting). **Catherine Cheung:** Conceptualization (supporting); Data curation (supporting); Formal analysis (supporting); Investigation (supporting); Methodology (supporting); Validation (supporting); Visualization (supporting); Writing – original draft (supporting); Writing – review & editing (supporting). **Yuna Heo:** Conceptualization (supporting); Data curation (supporting); Formal analysis (supporting); Investigation (supporting);

Methodology (supporting); Validation (supporting); Writing – original draft (supporting); Writing – review & editing (supporting). **Bat-Ider Tumenbayar:** Conceptualization (supporting); Data curation (supporting); Formal analysis (supporting); Investigation (supporting); Methodology (supporting); Visualization (supporting); Writing – original draft (supporting); Writing – review & editing (supporting). **Se-Hwan Lee:** Conceptualization (supporting); Data curation (supporting); Formal analysis (equal); Investigation (supporting); Methodology (supporting); Writing – original draft (supporting); Writing – review & editing (supporting). **Yongho Bae:** Formal analysis (supporting); Investigation (supporting); Validation (supporting); Writing – original draft (supporting); Writing – review & editing (supporting). **Su Chin Heo:** Conceptualization (lead); Formal analysis (equal); Funding acquisition (lead); Investigation (equal); Resources (equal); Supervision (lead); Writing – original draft (equal); Writing – review & editing (equal).

DATA AVAILABILITY

The data that support the findings of this study are available from the corresponding author upon reasonable request.

REFERENCES

[1]E. A. Makris, P. Hadidi, and K. A. Athanasiou, "The knee meniscus: Structure-function, pathophysiology, current repair techniques, and prospects for regeneration," Biomaterials **32**(30), 7411–7431 (2011).

[2]H. Kurosawa, T. Fukubayashi, and H. Nakajima, "Load-bearing mode of the knee joint: Physical behavior of the knee joint with or without menisci," Clin. Orthop. Relat. Res. **149**, 283–290 (1980).

[3]A. J. S. Fox, A. Bedi, and S. A. Rodeo, "The basic science of human knee menisci: Structure, composition, and function," Sports Health **4**(4), 340 (2012).

[4]M. Englund, F. W. Roemer, D. Hayashi, M. D. Crema, and A. Guermazi, "Meniscus pathology, osteoarthritis and the treatment controversy," Nat. Rev. Rheumatol. **8**(7), 412 (2012).

[5]D. J. Wyland, F. Guilak, D. M. Elliott, L. A. Setton, and T. P. Vail, "Chondropathy after meniscal tear or partial meniscectomy in a canine model," J. Orthop. Res. **20**(5), 996 (2002).

[6]M. Englund, A. Guermazi, F. W. Roemer, P. Aliabadi, M. Yang, C. E. Lewis, J. Torner, M. C. Nevitt, B. Sack, and D. T. Felson, "Meniscal tear in knees without surgery and the development of radiographic osteoarthritis among middle-aged and elderly persons: The multicenter osteoarthritis study," Arthritis Rheum. **60**(3), 831 (2009).

[7]S. C. Mordecai, N. Al-Hadithy, H. E. Ware, and C. M. Gupte, "Treatment of meniscal tears: An evidence based approach," World J. Orthop. **5**(3), 233 (2014).

[8]C. S. Shin and J. H. Lee, "Arthroscopic treatment for osteoarthritic knee," Knee Surg. Relat. Res. **24**(4), 187 (2012).

[9]C. Rangger, A. Kathrein, T. Klestil, and W. Glötzer, "Partial meniscectomy and osteoarthritis. Implications for treatment of athletes," Sports Med. **23**(1), 61 (1997).

[10]M. Bigoni, M. Turati, P. Sacerdote, D. Gaddi, M. Piatti, A. Castelnuovo, S. Franchi, M. Gandolla, A. Pedrocchi, R. J. Omeljaniuk, E. Bresciani, V. Locatelli, and A. Torsello, "Characterization of synovial fluid cytokine profiles in chronic meniscal tear of the knee," J. Orthop. Res. **35**(2), 340 (2017).

[11]A. Hennerbichler, F. T. Moutos, D. Hennerbichler, J. B. Weinberg, and F. Guilak, "Interleukin-1 and tumor necrosis factor alpha inhibit repair of the porcine meniscus *in vitro*," Osteoarthritis Cartilage **15**(9), 1053 (2007).

[12]S. Larsson, M. Englund, A. Struglics, and L. S. Lohmander, "Interleukin-6 and tumor necrosis factor alpha in synovial fluid are associated with progression of radiographic knee osteoarthritis in subjects with previous meniscectomy," Osteoarthritis Cartilage **23**(11), 1906 (2015).

[13]T. Ogura, M. Suzuki, Y. Sakuma, K. Yamauchi, S. Orita, M. Miyagi, T. Ishikawa, H. Kamoda, Y. Oikawa, I. Kanisawa, K. Takahashi, H. Sakai, T. Nagamine, H. Fukuda, K. Takahashi, S. Ohtori, and A. Tsuchiya, "Differences in levels of inflammatory mediators in meniscal and synovial tissue of patients with meniscal lesions," J. Exp. Orthop. **3**(1), 7 (2016).

[14]X. Du, Z. y. Liu, X. x. Tao, Y. l. Mei, D. q. Zhou, K. Cheng, S. l. Gao, H. y. Shi, C. Song, and X. m. Zhang, "Research progress on the pathogenesis of knee osteoarthritis," Orthop. Surg. **15**(9), 2213 (2023).

[15]P. Behrendt, K. Häfelein, A. Preusse-Prange, A. Bayer, A. Seekamp, and B. Kurz, "IL-10 ameliorates TNF-α induced meniscus degeneration in mature meniscal tissue in vitro," BMC Musculoskeletal Disord. **18**(1), 197 (2017).

[16]J. Melrose, S. Smith, M. Cake, R. Read, and J. Whitelock, "Comparative spatial and temporal localisation of perlecan, aggrecan and type I, II and IV collagen in the ovine meniscus: An ageing study," Histochem. Cell Biol. **124**(3–4), 225 (2005).

[17]C. A. Murphy, A. K. Garg, J. Silva-Correia, R. L. Reis, J. M. Oliveira, and M. N. Collins, "The meniscus in normal and osteoarthritic tissues: Facing the structure property challenges and current treatment trends," Annu. Rev. Biomed. Eng. **21**, 495 (2019).

[18]R. L. Mauck, G. J. Martinez-Diaz, X. Yuan, and R. S. Tuan, "Regional multilineage differentiation potential of meniscal fibrochondrocytes: Implications for meniscus repair," Anat. Rec. **290**(1), 48–58 (2007).

[19]K. Nakata, K. Shino, M. Hamada, T. Mae, T. Miyama, H. Shinjo, S. Horibe, K. Tada, T. Ochi, and H. Yoshikawa, "Human meniscus cell: Characterization of the primary culture and use for tissue engineering," Clin. Orthop. Relat. Res. **391**, S208 (2001).

[20]Z. Ma, M. J. Vyhlidal, D. X. Li, and A. B. Adesida, "Mechano-bioengineering of the knee meniscus," Am. J. Physiol. Cell Physiol. **323**(6), C1652 (2022).

[21]G. Bahcecioglu, B. Bilgen, N. Hasirci, and V. Hasirci, "Anatomical meniscus construct with zone specific biochemical composition and structural organization," Biomaterials **218**, 119361 (2019).

[22]L. Aidos, S. C. Modina, V. R. H. Millar, G. M. Peretti, L. Mangiavini, M. Ferroni, F. Boschetti, and A. Di Giancamillo, "Meniscus matrix structural and biomechanical evaluation: Age-dependent properties in a swine model," Bioengineering **9**(3), 117 (2022).

[23]L. Liu, Q. Luo, J. Sun, Y. Ju, Y. Morita, and G. Song, "Chromatin organization regulated by EZH_2-mediated $H_3K_{27}me_3$ is required for OPN-induced migration of bone marrow-derived mesenchymal stem cells," Int. J. Biochem. Cell Biol. **96**, 29–39 (2018).

[24]G. Gerlitz and M. Bustin, "Efficient cell migration requires global chromatin condensation," Development **137**(14), e1 (2010).

[25]G. Gerlitz and M. Bustin, "The role of chromatin structure in cell migration," Trends Cell Biol. **21**(1), 6 (2011).

[26]S. J. Heo, K. H. Song, S. Thakur, L. M. Miller, X. Cao, A. P. Peredo, B. N. Seiber, F. Qu, T. P. Driscoll, V. B. Shenoy, M. Lakadamyali, J. A. Burdick, and R. L. Mauck, "Nuclear softening expedites interstitial cell migration in fibrous networks and dense connective tissues," Sci. Adv. **6**, eaax5083 (2020).

[27]G. Gerlitz, "The emerging roles of heterochromatin in cell migration," Front. Cell Dev. Biol. **8**, 394 (2020).

[28]S.-J. Heo, S. Thakur, X. Chen, C. Loebel, B. Xia, R. McBeath, J. A. Burdick, V. B. Shenoy, R. L. Mauck, and M. Lakadamyali, "Aberrant chromatin reorganization in cells from diseased fibrous connective tissue in response to altered chemomechanical cues," Nat. Biomed. Eng. **7**, 177 (2022).

[29]M. A. Ricci, C. Manzo, M. F. García-Parajo, M. Lakadamyali, and M. P. Cosma, "Chromatin fibers are formed by heterogeneous groups of nucleosomes in vivo," Cell **160**(6), 1145–1158 (2015).

[30]M. Yamagishi, M. Hori, D. Fujikawa, T. Ohsugi, D. Honma, N. Adachi, H. Katano, T. Hishima, S. Kobayashi, K. Nakano, M. Nakashima, M. Iwanaga, A. Utsunomiya, Y. Tanaka, S. Okada, K. Tsukasaki, K. Tobinai, K. Araki, T. Watanabe, and K. Uchimaru, "Targeting excessive EZH1 and EZH2 activities for abnormal histone methylation and transcription network in malignant lymphomas," Cell Rep. **29**(8), 2321 (2019).

[31]H. Fan, H. I. Atiya, Y. Wang, T. R. Pisanic, T. H. Wang, I. M. Shih, K. K. Foy, L. Frisbie, R. J. Buckanovich, A. A. Chomiak, R. L. Tiedemann, S. B. Rothbart, C. Chandler, H. Shen, and L. G. Coffman, "Epigenomic reprogramming toward mesenchymal-epithelial transition in ovarian-cancer-associated mesenchymal stem cells drives metastasis," Cell Rep. **33**(10), 108473 (2020).

[32]P. Das and J. H. Taube, "Regulating methylation at H3K27: A trick or treat for cancer cell plasticity," Cancers **12**(10), 2792 (2020).

[33]H. Cardenas, J. Zhao, E. Vieth, K. P. Nephew, and D. Matei, "EZH2 inhibition promotes epithelial-to-mesenchymal transition in ovarian cancer cells," Oncotarget **7**(51), 84453 (2016).
[34]K. M. Riera, N. E. Rothfusz, R. E. Wilusz, J. B. Weinberg, F. Guilak, and A. L. McNulty, "Interleukin-1, tumor necrosis factor-alpha, and transforming growth factor-beta 1 and integrative meniscal repair: Influences on meniscal cell proliferation and migration," Arthritis Res. Ther. **13**(6), R187 (2011).
[35]M. M. Pillai, V. Elakkiya, J. Gopinathan, C. Sabarinath, S. Shanthakumari, K. S. Sahanand, B. K. Dinakar Rai, A. Bhattacharyya, and R. Selvakumar, "A combination of biomolecules enhances expression of E-cadherin and peroxisome proliferator-activated receptor gene leading to increased cell proliferation in primary human meniscal cells: An in vitro study," Cytotechnology **68**(5), 1747 (2016).
[36]U. Freymann, S. Metzlaff, J. P. Krüger, G. Hirsh, M. Endres, W. Petersen, and C. Kaps, "Effect of human serum and 2 different types of platelet concentrates on human meniscus cell migration, proliferation, and matrix formation," Arthroscopy **32**(6), 1106 (2016).
[37]C. Doñas, M. Carrasco, M. Fritz, C. Prado, G. Tejón, F. Osorio-Barrios, V. Manríquez, P. Reyes, R. Pacheco, M. R. Bono, A. Loyola, and M. Rosemblatt, "The histone demethylase inhibitor GSK-J4 limits inflammation through the induction of a tolerogenic phenotype on DCs," J. Autoimmun. **75**, 105 (2016).
[38]K. Xu, X. Liu, B. Wen, Y. Liu, W. Zhang, X. Hu, L. Chen, W. Hang, and J. Chen, "GSK-J4, a specific histone lysine demethylase 6A inhibitor, ameliorates lipotoxicity to cardiomyocytes via preserving H3K27 methylation and reducing ferroptosis," Front. Cardiovasc. Med. **9**, 907747 (2022).
[39]T. L. Lochmann, K. M. Powell, J. Ham, K. V. Floros, D. A. R. Heisey, R. I. J. Kurupi, M. L. Calbert, M. S. Ghotra, P. Greninger, M. Dozmorov, M. Gowda, A. J. Souers, C. P. Reynolds, C. H. Benes, and A. C. Faber, "Targeted inhibition of histone H3K27 demethylation is effective in high-risk neuroblastoma," Sci. Transl. Med. **10**(441), eaao4680 (2018).
[40]N. Dalpatraj, A. Naik, and N. Thakur, "GSK-J4: An H3K27 histone demethylase inhibitor, as a potential anti-cancer agent," Int. J. Cancer **153**(6), 1130 (2023).
[41]G. Yan, M. S. Eller, C. Elm, C. A. Larocca, B. Ryu, I. P. Panova, B. M. Dancy, E. M. Bowers, D. Meyers, L. Lareau, P. A. Cole, S. D. Taverna, and R. M. Alani, "Selective inhibition of p300 HAT blocks cell cycle progression, induces cellular senescence, and inhibits the DNA damage response in melanoma cells," J, Invest. Dermatol. **133**(10), 2444 (2013).
[42]Y. M. Wang, M. L. Gu, F. S. Meng, W. R. Jiao, X. X. Zhou, H. P. Yao, and F. Ji, "Histone acetyltransferase p300/CBP inhibitor C646 blocks the survival and invasion pathways of gastric cancer cell lines," Int. J. Oncol. **51**(6), 1860 (2017).
[43]X. N. Gao, J. Lin, Q. Y. Ning, L. Gao, Y. S. Yao, J. H. Zhou, Y. H. Li, L. L. Wang, and L. Yu, "A histone acetyltransferase p300 inhibitor C646 induces cell cycle arrest and apoptosis selectively in AML1-ETO-positive AML cells," PLoS One **8**(2), e55481 (2013).
[44]S. Tarafder, G. Park, and C. H. Lee, "Explant models for meniscus metabolism, injury, repair, and healing," Connect. Tissue Res. **61**(3–4), 292 (2020).
[45]A. L. McNulty, F. T. Moutos, J. B. Weinberg, and F. Guilak, "Enhanced integrative repair of the porcine meniscus in vitro by inhibition of interleukin-1 or tumor necrosis factor α," Arthritis Rheum. **56**(9), 3033 (2007).
[46]R. E. Wilusz, J. B. Weinberg, F. Guilak, and A. L. McNulty, "Inhibition of integrative repair of the meniscus following acute exposure to interleukin-1 in vitro," J. Orthop. Res. **26**(4), 504 (2008).
[47]T. Murakami, S. Otsuki, Y. Okamoto, K. Nakagawa, H. Wakama, N. Okuno, and M. Neo, "Hyaluronic acid promotes proliferation and migration of human meniscus cells via a CD44-dependent mechanism," Connect. Tissue Res. **60**(2), 117–127 (2019).
[48]K. Blighe, S. Rana, and M. Lewis, "EnhancedVolcano version 1.10.0: Publication-ready volcano plots with enhanced colouring and labeling," R-Package (2021).
[49]S. H. Lee, O. Kim, H. J. Kim, C. Hwangbo, and J. H. Lee, "Epigenetic regulation of TGF-β-induced EMT by JMJD3/KDM6B histone H3K27 demethylase," Oncogenesis **10**(2), 17 (2021).
[50]L. Qu, T. Yin, Y. Zhao, W. Lv, Z. Liu, C. Chen, K. Liu, S. Shan, R. Zhou, X. Li, and H. Dong, "Histone demethylases in the regulation of immunity and inflammation," Cell Death Discovery **9**(1), 188 (2023).
[51]C. Doñas, J. Neira, F. Osorio-Barrios, M. Carrasco, D. Fernández, C. Prado, A. Loyola, R. Pacheco, and M. Rosemblatt, "The demethylase inhibitor GSK-J4 limits inflammatory colitis by promoting de novo synthesis of retinoic acid in dendritic cells," Sci. Rep. **11**(1), 1342 (2021).
[52]T. Van Den Bosch, A. Boichenko, N. G. J. Leus, M. E. Ourailidou, H. Wapenaar, D. Rotili, A. Mai, A. Imhof, R. Bischoff, H. J. Haisma, and F. J. Dekker, "The histone acetyltransferase p300 inhibitor C646 reduces pro-inflammatory gene expression and inhibits histone deacetylases," Biochem. Pharmacol. **102**, 130 (2016).
[53]F. Fang, G. Li, M. Jing, L. Xu, Z. Li, M. Li, C. Yang, Y. Liu, G. Qian, X. Hu, G. Li, Y. Xie, C. Feng, X. Li, J. Pan, Y. Li, X. Feng, and Y. Li, "C646 modulates inflammatory response and antibacterial activity of macrophage," Int. Immunopharmacol. **74**, 105736 (2019).
[54]H. Sun, X. Wen, H. Li, P. Wu, M. Gu, X. Zhao, Z. Zhang, S. Hu, G. Mao, R. Ma, W. Liao, and Z. Zhang, "Single-cell RNA-seq analysis identifies meniscus progenitors and reveals the progression of meniscus degeneration," Ann. Rheum. Dis. **79**(3), 408 (2020).
[55]J. Wang, S. Roberts, J. H. Kuiper, W. Zhang, J. Garcia, Z. Cui, and K. Wright, "Characterization of regional meniscal cell and chondrocyte phenotypes and chondrogenic differentiation with histological analysis in osteoarthritic donor-matched tissues," Sci. Rep. **10**(1), 21658 (2020).
[56]M. I. Love, W. Huber, and S. Anders, "Moderated estimation of fold change and dispersion for RNA-seq data with DESeq2," Genome Biol. **15**(12), 550 (2014).
[57]R. Kolde, "Package 'pheatmap': Pretty heatmaps," R Package (2022).
[58]J. Reimand, M. Kull, H. Peterson, J. Hansen, and J. Vilo, "G:Profiler-a web-based toolset for functional profiling of gene lists from large-scale experiments," Nucl. Acids Res. **35**(SUPPL.2), W193 (2007).
[59]H. Wickham, *Ggplot2: Elegant Graphics for Data Analysis* (Springer-Verlag New York, 2016).
[60]J. Otterstrom, A. Castells-Garcia, C. Vicario, P. A. Gomez-Garcia, M. P. Cosma, and M. Lakadamyali, "Super-resolution microscopy reveals how histone tail acetylation affects DNA compaction within nucleosomes *in vivo*," Nucl. Acids Res. **47**, 117–127 (2019).